

# Self-Organization of Zr(IV) Porphyrinoids on Graphene Oxide Surfaces by Axial Metal Coordination

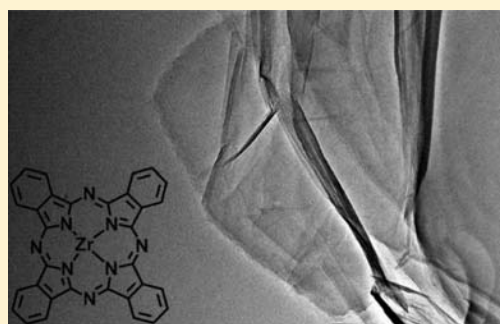
Matthew Jurow,<sup>†</sup> Viacheslav Manichev,<sup>||,†</sup> Cesar Pabon,<sup>||,†</sup> Brian Hageman,<sup>†</sup> Yuliya Matolina,<sup>†</sup> and Charles Michael Drain<sup>\*,†,‡</sup>

<sup>†</sup>Department of Chemistry and Biochemistry, Hunter College of the City University of New York, 695 Park Avenue, New York, New York 10021, United States

<sup>‡</sup>Rockefeller University, 1230 York Avenue, New York, New York 10065, United States

## S Supporting Information

**ABSTRACT:** The protruding oxophilic central metal ion of Zr<sup>IV</sup> porphyrinoids facilitates axial coordination to the oxygen bearing functional groups on graphene oxide (GO) surfaces to result in new supramolecular photonic materials with high dye loading especially on edges and large defects. The reaction proceeds at room temperature with GO dispersed in tetrahydrofuran and GO films on glass. Since the Zr<sup>IV</sup> serves as a conduit, the photophysical properties of the dye sensitized GO derive from both the axially bound chromophores and the GO substrate. Self-organization of metalloporphyrinoids on GO mediated by axial coordination of group (IV) metal ions allows for direct sensitization of graphene and graphenic materials without requiring covalent chemistries with poorly conducting linkers.



## INTRODUCTION

The unique properties of graphene oxide (GO) have driven research on using GO in functional materials for diverse applications.<sup>1–4</sup> GO is produced by a variety of scalable methods that result in similar, but not identical, products.<sup>5</sup> Theories about the exact structure of GO have continuously evolved because of the nonhomogenous nature of the material.<sup>6</sup> A commonly accepted model (Lerf–Klinowski) describes a surface composed of a substituted network of sp<sup>2</sup> and sp<sup>3</sup> hybridized carbon atoms. Alcohol and epoxide functionalities are present on the basal planes with carboxylic groups along the edges and larger defect sites of the flakes, which range between tens of nanometers and tens of micrometers in edge length and 0.8–1.5 nm in thickness if fully exfoliated depending on the method of production.<sup>7</sup>

Interest in GO has focused on properties arising from its nonstoichiometric nature resulting in regions of variable oxygen content, controllable dispersibility in water and organic solvents,<sup>8</sup> interesting photonic properties,<sup>9</sup> and potential for use in biological systems such as for photodynamic therapeutics and for drug delivery.<sup>1,10–14</sup> Recent reports demonstrate GO applications in nonlinear optics,<sup>15</sup> as *p* or *n* type materials,<sup>16,17</sup> as a functional surfactant,<sup>18</sup> as antennae complexes to collect solar energy, and as efficient catalysts.<sup>19</sup>

Free base and metallotetraphenylporphyrins can be covalently bound to GO via amides<sup>20,21</sup> and esters,<sup>22,23</sup> or deposited by molecular beam<sup>24</sup> to yield photonic materials. Cationic porphyrins electrostatically associate with GO and rGO, and GO can be appended with polyethylene glycols to make biocompatible materials.<sup>10,11</sup> Large, planar phthalocyanines and their metal derivatives associate with graphene and areas in

reduced graphene oxide (rGO) via  $\pi$ – $\pi$  interactions.<sup>25–27</sup> Sensitized hybrid GO materials can serve as components of solar cell devices,<sup>28–30</sup> and electrodes.<sup>31</sup>

We report herein the efficient self-organization and photonic properties of materials composed of 5,10,15,20-tetraphenylporphyrinato Zr<sup>IV</sup>, Zr<sup>IV</sup>(TPP), or phthalocyaninato Zr<sup>IV</sup>, Zr<sup>IV</sup>(Pc) (Figure 1) on graphene oxide, GO. The 7–8 coordinate oxophilic Zr<sup>IV</sup> ions protrude from one face of the Zr<sup>IV</sup>(TPP) and the Zr<sup>IV</sup>(Pc) so that they are available to strongly coordinate to the bidentate acetates or oxygen containing functional groups on the surfaces and edges of GO. The supramolecular material is assembled from dyes with acetates as auxiliary ligands, Zr<sup>IV</sup>(TPP)Ac<sub>2</sub> and Zr<sup>IV</sup>(Pc)Ac<sub>2</sub>, which are easily synthesized in good yields from commercially available precursors and have electronic spectra typical of metalloporphyrins and metallophthalocyanines, respectively.<sup>32,33</sup> The large ionic radius of Zr<sup>IV</sup>, 0.72 Å, results in an unusual 0.9 Å to 1 Å displacement from the mean plane of the macrocycle nitrogen atoms, thereby enabling group IV metalloporphyrinoids to simultaneously bind oxygen groups on materials such as defects in polyoxometalates and to TiO<sub>2</sub> surfaces used in dye sensitized solar cells.<sup>33–35</sup> In contrast, Zn<sup>II</sup> resides in the mean plane of the Pc and TPP macrocycles and is weakly six coordinate, thus Zn(TPP) and Zn(Pc) (Figure 1) do not strongly interact with GO and are used as control dyes for comparison of the photonic properties of the dye-sensitized GO materials.

Received: June 19, 2013

Published: September 5, 2013

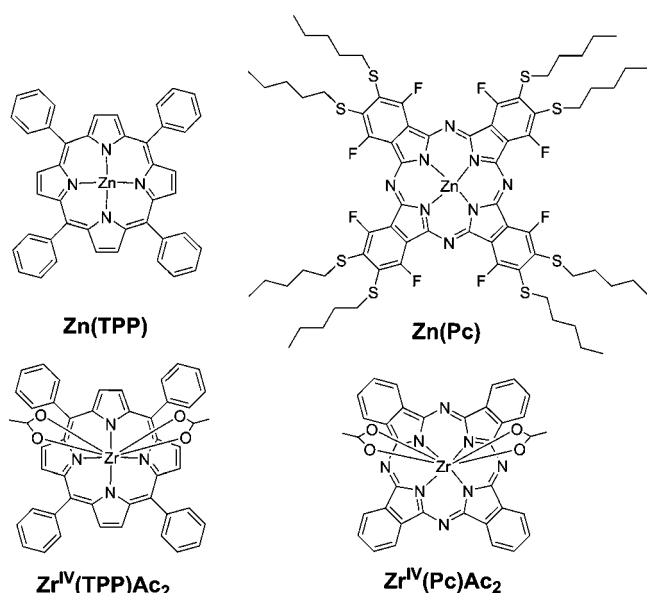


**Figure 1.** Since the 8-coordinate  $Zr^{IV}$  ion protrudes from one face of the *S*,*10*,*15*,*20*-tetraphenylporphyrin (TPP) and phthalocyanine (Pc) the  $Zr^{IV}$  axially coordinates GO by replacement of bidentate acetate groups with oxygen groups on the GO (bottom). The 4-coordinate Zn analogue very weakly accepts axial ligands and does not bind GO (top).

Direct attachment of the chromophore to the GO surface via the protruding metal ion results in a coplanar orientation of the chromophores relative to the GO surface and at an angle on the edges and large defects. Some plausible geometries derived from MM2 calculations are suggested in Figure 2, and are consistent with  $Zr^{IV}(\text{TPP})$  and  $Zr^{IV}(\text{Pc})$  bound to a defect site in a polyoxometalate.<sup>33,35</sup> In contrast to covalent chemistry, this supramolecular chemistry approach increases the efficiency of dye loading, strongly couples the electronic properties of the two components, and preserves the properties of the substrate.

The  $Zr^{IV}$  serves as a direct conduit for electronic coupling of the dye and GO systems because of the mixing of the metal ion and chromophore orbitals.<sup>15,36</sup> The photonic properties of this new hybrid material can be tuned by altering the photophysical properties of the dye, and represents an avenue for the development of a variety of sensitized graphenic materials.

## MATERIALS AND METHODS

Atomic Force Microscopy (AFM) measurements were conducted with an Asylum Research Corp. (MFP-3D) or an Agilent 5500 instrument using standard n-type silicon cantilevers with reflective aluminum coating (MikroMasch NSC15-AIBS) with a nominal spring constant of 40 N/m and frequency of 325 kHz, at a scan rate of 15  $\mu\text{m}/\text{sec}$ . UV–visible absorption spectroscopy was performed on a Cary 1-Bio UV–visible spectrometer. Steady state fluorescence spectra were obtained on a HORIBA Jobin-Yvon FluoroLog-3 fluorometer. Quartz or optical glass cuvettes were used for all spectroscopic studies. All photophysical studies were carried out in distilled solvents. MM2 calculations were done in Chem3D. Experiments have been repeated multiple times by at least three different researchers.

$Zn(\text{Pc})$  is synthesized by simple click-type substitution of peripheral fluorine atoms on the commercially available perfluorophthalocyanine precursor with thioalkanes to improve solubility.<sup>37</sup> Synthetic details of  $Zr^{IV}$  dyes are reported.<sup>33,35</sup> GO material was purchased from Graphene Supermarket who report that the material is >60% single layer, flakes are 0.5–5  $\mu\text{m}$ , and with 20% oxygen (w/w).

**Optical Spectra.** A dispersion of 0.1 mg/mL GO is made by sonicating single layer GO flakes in freshly distilled (THF),<sup>38</sup> and titrated in 40  $\mu\text{L}$  aliquots into 3 mL solutions of 3  $\mu\text{M}$   $Zr^{IV}(\text{Pc})\text{Ac}_2$  or 2  $\mu\text{M}$   $Zr^{IV}(\text{TPP})\text{Ac}_2$  in THF. After 24 h to allow the dyes to bind the GO, the UV–visible and fluorescence emission spectra were recorded in 1  $\times$  1 cm cuvettes ( $\lambda_{\text{ex}}$ : 655 nm for  $Zn(\text{Pc})$ , 633 nm for  $Zr^{IV}(\text{Pc})$ , 422 nm for  $Zn(\text{TPP})$ , and 417 nm for  $Zr^{IV}(\text{TPP})$ ). Fluorescence quenching comparisons were recorded at consistent absorbance values.

**Nanocomposites.** GO was added to 100  $\mu\text{M}$  solutions of  $Zr^{IV}(\text{Pc})\text{Ac}_2$  or  $Zr^{IV}(\text{TPP})\text{Ac}_2$  in THF to make a 0.1 mg/mL GO solution, and sonicated for 5 min to ensure good dispersion. After allowing 48 h for equilibration at room temperature, samples were centrifuged at 13,000 rpm for 15 min and washed twice with fresh THF to remove unbound dye molecules.

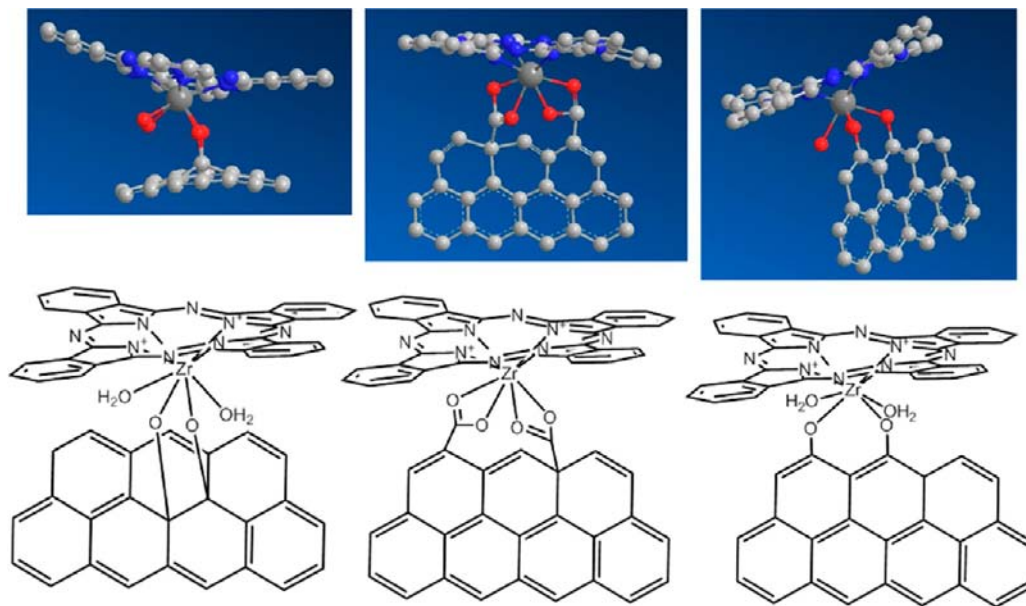


**Figure 2.** Three ways of binding of  $Zr^{IV}(\text{Pc})$  on a small region of GO are representative of the several possible binding modes. The  $Zr^{IV}(\text{TPP})$  bind similarly. Three-dimensional renderings are approximated from MM2 calculations (top, left to right) for internal diol, side carboxylates, and side diols; gray, C; blue, N; red, O; dark gray,  $Zr^{IV}$ ; H left out for clarity.

**AFM.** Samples for AFM were prepared either by dip coating ozone cleaned glass into the suspensions of the nanocomposites in THF or by centrifuging the suspension, dispersing the pellet into nanopure water by sonication, and spin coating onto ozone cleaned glass.

**TEM.** All data were collected at 200 kV on a Jeol 2100 transmission electron microscope equipped with EDAX at the eucentric point to ensure reproducibility of the measurements. An 8  $\mu\text{L}$  drop of the above nanocomposite dispersion was placed on a 300 mesh carbon coated copper grid (TED Pella Inc.) and allowed to dry for 1 min before imaging.

**Films.** GO in aqueous suspension (3 mg/mL) was spin coated onto piranha cleaned quartz slides and dried in an oven to make 15 nm thick continuous films. Films were then soaked in 0.1 mM solutions of dyes in  $\text{CH}_2\text{Cl}_2$  for three days at room temperature in the dark to ensure equilibration. The films were rinsed extensively with clean  $\text{CH}_2\text{Cl}_2$  to remove any unbound dye, and the backs of the slides were cleaned repeatedly with MeOH before spectra were recorded.

**Probe Measurements.** Devices were made by spin coating layers of GO (of 8 or 15 nm) onto ozone cleaned glass from an aqueous suspension. Sheet resistance was measured by Van der Pauw technique of the pristine GO layers, of an 8 nm GO film soaked in  $\text{Zr}^{\text{IV}}(\text{Pc})$  or  $\text{Zr}^{\text{IV}}(\text{TPP})$  (0.1 mM in  $\text{CH}_2\text{Cl}_2$ ), or of an 8 nm GO film spin coated on top of an about 40 nm thick layer of  $\text{Zr}^{\text{IV}}(\text{TPP})$  or  $\text{Zr}^{\text{IV}}(\text{Pc})$  spin-cast from chlorobenzene on ozone cleaned glass. Measurements were taken in the dark and under illumination.

## RESULTS AND DISCUSSION

GO dispersions in THF were added to solutions of  $\text{Zr}^{\text{IV}}(\text{Pc})\text{Ac}_2$  or  $\text{Zr}^{\text{IV}}(\text{TPP})\text{Ac}_2$  and allowed to react for 24 h to allow the maximal amount of the  $\text{Zr}^{\text{IV}}(\text{Pc})$  or  $\text{Zr}^{\text{IV}}(\text{TPP})$  to bind to GO. These are similar conditions used to bind the  $\text{Zr}^{\text{IV}}$  metal-porphyrinoids to surface oxygens on nanoparticles of  $\text{TiO}_2$ .<sup>34</sup> The UV-visible spectral shifts and decreased intensity in the  $\text{Zr}^{\text{IV}}(\text{Pc})$  Q-band (676 nm) and  $\text{Zr}^{\text{IV}}(\text{TPP})$  Soret (421 nm) after incubation are consistent with displacement of the acetate ligands by the oxygen functional groups on the GO and formation of the hybrid material (Figure 3).<sup>34</sup> The intensity of the UV-visible spectra of the hybrid materials with  $\text{Zr}^{\text{IV}}(\text{Pc})$  or  $\text{Zr}^{\text{IV}}(\text{TPP})$  attached to GO monotonically decreases without changes in peak  $\lambda_{\text{max}}$  as the solution is diluted, thus indicating that the solution is homogeneously dissolved and the zirconium dyes are strongly bound to the GO. Since the zinc species,  $\text{Zn}(\text{Pc})$  and  $\text{Zn}(\text{TPP})$ , cannot accommodate further ligation and do not chemically bond GO, the electronic spectra are not altered upon addition of the GO dispersion.

Significant fluorescence quenching of the  $\text{Zr}^{\text{IV}}$  dyes indicates charge injection from the chromophore excited state (HOMO  $-5.4$  eV, LUMO  $-3.6$  eV, band gap 1.8 eV)<sup>34</sup> into the GO made possible by the large band gap of GO (ca.  $-5.6$  eV to  $-4.0$  eV).<sup>20,39-41</sup> When binding is complete, the emission is quenched by 70% for the  $\text{Zr}^{\text{IV}}(\text{Pc})$  and 30% for the  $\text{Zr}^{\text{IV}}(\text{TPP})$ , respectively. The quenching is consistent with electron transfer to the GO as found with covalently bound porphyrinoids to graphene and GO.<sup>4</sup> Note that the peripheral phenyl groups on TPP are nominally orthogonal to the macrocycle with dihedral angles of  $90 \pm 20^\circ$ , thus the phenyl moieties on  $\text{Zr}^{\text{IV}}(\text{TPP})$  likely reduce binding to the surfaces of GO by steric hindrance. For  $\text{Zn}(\text{TPP})$  and  $\text{Zn}(\text{Pc})$  controls, the electronic absorption and emission spectra are unchanged by addition of the GO dispersion, indicating no interaction. Note that the large Stokes shift for the  $\text{Zr}^{\text{IV}}(\text{Pc})$  is typical for these compounds.

To investigate the properties of the material in the solid state, films of GO were spin-cast onto quartz substrates from dispersions in water, soaked in 0.1 mM dye solutions in  $\text{CH}_2\text{Cl}_2$  for 72 h, and rinsed thoroughly with clean solvent. An aqueous

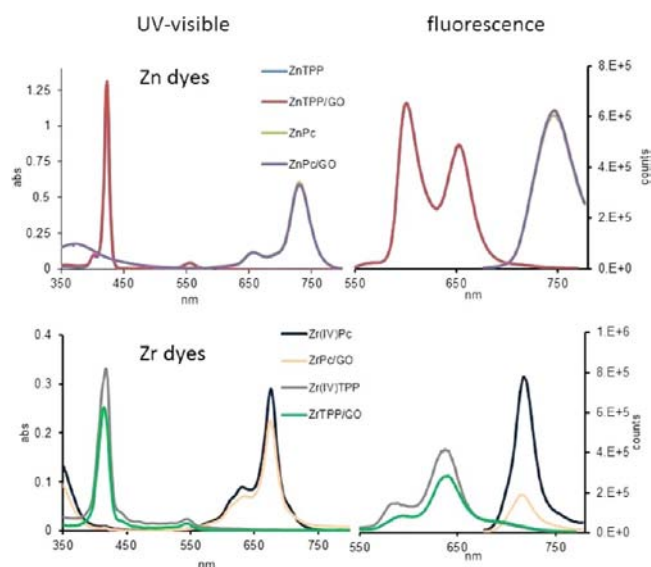


**Figure 3.** Top: the UV-visible and fluorescence spectra of the Zn dyes overlap with the spectra after addition of 120  $\mu\text{L}$  of 0.1 mg/mL GO dispersed in THF; indicating that neither  $\text{ZnPc}$  nor  $\text{Zn}(\text{TPP})$  interact with GO. Bottom: the significant changes in the UV-visible and fluorescence quenching of  $\text{Zr}^{\text{IV}}(\text{TPP})\text{Ac}_2$  and  $\text{Zr}^{\text{IV}}(\text{Pc})\text{Ac}_2$  after addition of 120  $\mu\text{L}$  of 0.1 mg/mL GO dispersed in THF indicate exchange of the acetate ligands for oxygen functional groups on the GO and binding of the metallo dyes.  $\lambda_{\text{ex}} = 417$  nm for  $\text{Zr}^{\text{IV}}(\text{TPP})$  and  $\text{Zn}(\text{TPP})$ ,  $\lambda_{\text{ex}} = 633$  nm for  $\text{Zn}(\text{Pc})$  and  $\text{Zr}^{\text{IV}}(\text{Pc})$ , in each case the optical density was  $<0.1$ .

GO dispersion of 3 mg/mL yielded 15 nm thick continuous films while a 1 mg/mL dispersion yielded an 8 nm film. After soaking in solutions of the  $\text{Zr}^{\text{IV}}(\text{TPP})\text{Ac}_2$  or  $\text{Zr}^{\text{IV}}(\text{Pc})\text{Ac}_2$  and rinsing well with fresh THF, fluorescence quenching by charge transfer from Zr containing dyes to GO is observed for these metal-coordinated films (Figure 4).<sup>42</sup> UV-visible spectra demonstrate the presence of the coordinated dyes on the GO films by the absorbance from the  $\text{Zr}^{\text{IV}}(\text{TPP})$  Soret (421 nm) and  $\text{Zr}^{\text{IV}}(\text{Pc})$  Q (693 nm) bands (Figure 4). The small peaks from the control  $\text{Zn}^{\text{II}}$  complexes are likely the result of dye molecules interacting with the GO in graphene like regions through  $\pi$ - $\pi$  interactions.

The absence of significant shifts in the optical spectra indicate that the dye molecules are not aggregated. Optical data on the films suggests a surface density<sup>43</sup> of about one chromophore per 20–50  $\text{nm}^2$ , assuming average flakes of 1  $\mu\text{m}^2$  and dyes bound to only one face. The C:Zr mole ratio obtained by elemental analysis (31:0.006) of the  $\text{Zr}^{\text{IV}}(\text{TPP})$  and  $\text{Zr}^{\text{IV}}(\text{Pc})$  bound to GO indicated similar packing densities of about one per 40  $\text{nm}^2$ . Collectively, these data indicate that the high oxygen content of the GO facilitates tight binding and high surface coverage of the  $\text{Zr}^{\text{IV}}$  dyes mediated by axial coordination.

In a separate experiment,  $\text{Zr}^{\text{IV}}(\text{Pc})\text{Ac}_2$  was added to a 0.1 mg/mL GO dispersion in THF to make solutions 100  $\mu\text{M}$  in dye and ensure saturation of the GO surfaces with  $\text{Zr}^{\text{IV}}$  chromophores. Suspensions were allowed to react about 72 h to reach equilibrium, whereupon the mixture was centrifuged, rinsed with clean THF to remove unbound dye, and dispersed again in THF by brief sonication to form nanocomposites of GO with  $\text{Zr}^{\text{IV}}(\text{Pc})$  coordinated to the protruding oxygen containing surface and edge groups. Ozone cleaned glass slides were dip coated into these dispersions and rinsed well with

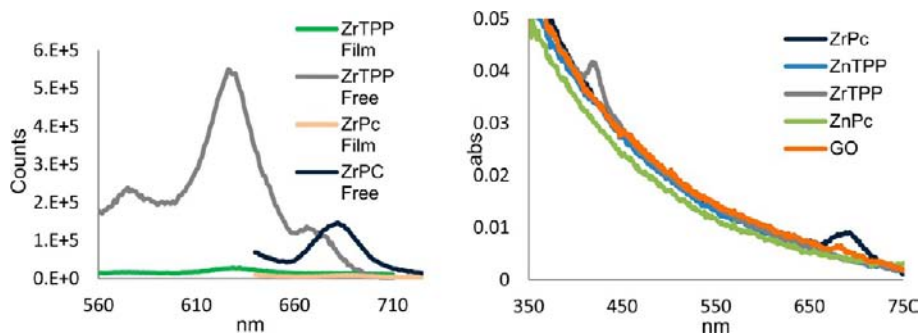


**Figure 4.** Left: fluorescence of  $Zr^{IV}(Pc)$  and  $Zr^{IV}(TPP)$  dyes bound to an about 15 nm thick film of GO is quenched compared to solutions of the unbound dyes with the same optical density.  $\lambda_{ex} = 417$  nm for  $Zr^{IV}(TPP)$  and 633 nm for  $Zr^{IV}(Pc)$ . Right: UV-visible spectra of the same GO films where control Zn dyes are not observed to bind the GO films.

clean THF. AFM analyses of these composite films confirm that the large oxygen:carbon ratio of the GO allows for high surface density of the coordinatively bound chromophores. Sonication in THF selectively removes dye molecules coordinated on the basal plane of the GO while preserving those coordinated more strongly to the flake edges, where there is a greater concentration of carboxylic groups<sup>44</sup> (Figure 5). A single

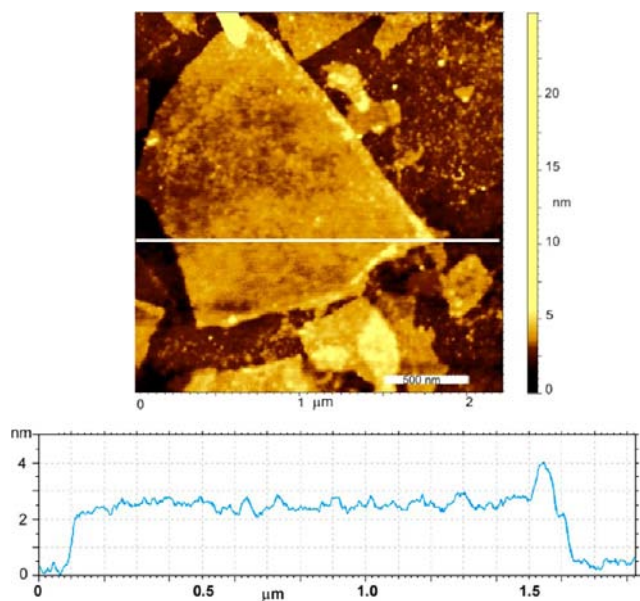


**Figure 5.** AFM image and height trace of about 2.8 nm high GO flake coated on both sides with  $Zr^{IV}(Pc)$  cast onto an ozone cleaned glass coverslip. Higher dye loading on GO edge is visible.

flake of GO is about 1.2 nm thick (Supporting Information, Figures S8, S9),<sup>45,46</sup> and single layer flakes of GO coated on both sides with  $Zr^{IV}(Pc)$  are observed, corresponding to heights of about 2.8 nm. The total heights of the  $Zr^{IV}(Pc)/GO$  composite correspond well to those predicted by adding the heights of the GO with the thickness of the dye obtained from crystal structures (Figure 5, Supporting Information, Figure S10).<sup>33</sup> The AFM of control samples prepared by identical methods using  $Zn(Pc)$  and  $Zn(TPP)$  show about 1.1 nm flakes of GO, and the absence of the zinc dyes.

TEM images of the same nanocomposites indicate a uniform coating of the GO surface with  $Zr^{IV}(Pc)$ , and EDAX spectra display characteristic bands for the presence of Zr (Figure 6, Supporting Information, Figure S7). No evidence of Zn is

observed by EDAX when GO is mixed with  $Zn(Pc)$  under the same conditions.

When the  $Zr^{IV}(Pc)/GO$  nanocomposites were centrifuged and redispersed in water, the nanocomposites precipitate rapidly, whereas the unfunctionalized GO remains suspended. This indicates a significantly increased hydrophobicity of the hybrid material relative to GO arising from the organic dye covering the face, and the lack of exposed oxygen species. Similar results are observed for the  $Zr^{IV}(TPP)$  on GO. To assess the robustness of the  $Zr^{IV}$  dye binding to the GO, the composite was sonicated (60 W, 30 min), and the solution was spin-cast onto ozone cleaned glass coverslips. AFM of films of these samples display perforations of the graphene flakes resultant from removal of the oxophilic  $Zr^{IV}(Pc)$  or  $Zr^{IV}(TPP)$  (Supporting Information, Figure S11). The perforation/degradation of the GO sheets also eliminates the fluorescence of the pristine GO flakes, and no fluorescence was observed for the dyes.<sup>9,47</sup> Control experiments with  $Zn(Pc)$  and GO display the characteristic UV-visible spectrum and broad fluorescence of GO without perforations. In a separate control experiment GO dispersions in THF were reacted with  $ZrCl_4$ . Large aggregates of metal ion cross-linked or intercalated GO sheets precipitate immediately. When dispersed by sonication into water no perforation or changes to the flakes are observed.

Four point probe measurements (Supporting Information, Table S1) yielded sheet resistance values of  $2.9 \times 10^{10}$  and  $3.6 \times 10^9 \Omega/\square$  for 8 and 15 nm thick GO films, respectively.<sup>48</sup> For composite films, made by spin-casting the  $Zr^{IV}(\text{dye})$  treated GO or dipping the cast GO into  $Zr^{IV}(Pc)$  or  $Zr^{IV}(TPP)$  solutions, the sheet resistance of 8 nm films decreased by about 50%. This indicates the  $Zr^{IV}$  dyes can bridge some of the defects in the GO material, thereby increasing conductivity. Future work will investigate the properties of the dye/substrate interface as well as anticipated doping and photoconductivity applications.<sup>8,16,49,50</sup>

Layer-by-layer assembly is a simple technique to create functional materials with controlled size, morphology, and physical properties on different substrates.<sup>51</sup> Films were made by sequential dipping of quartz slides with an 8 nm GO layer into solutions of  $Zn(Pc)$ ,  $Zr^{IV}(Pc)$ , or  $ZrCl_4$  (Figure 7, Supporting Information, Figures S13–16). Initially, the hydroxyl groups on the GO flakes associate with the quartz substrate, likely by hydrogen bonding.<sup>52</sup> The nonstoichiometric nature, oxidative debris, and varied size of the GO flakes result in imperfections and varied coverage in the initial layer, but these are filled as the films develop in thickness.  $Zn(Pc)$  adheres to any hydrophobic basal plane regions of unoxidized  $sp^2$

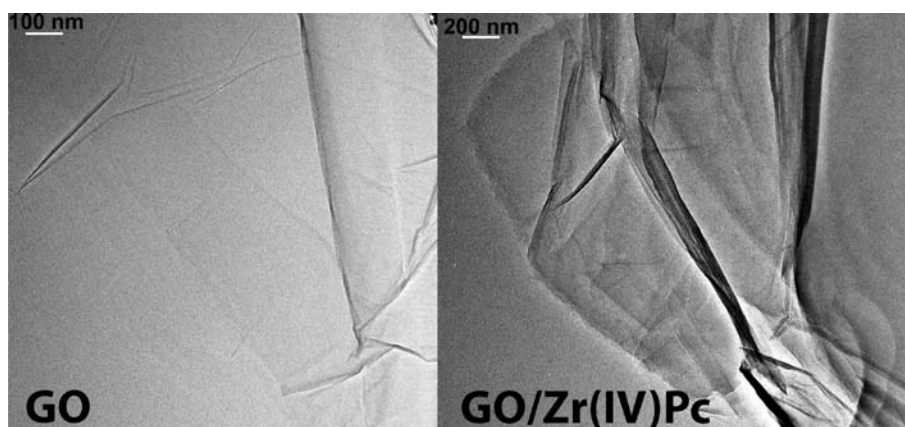


**Figure 6.** TEM images of GO flakes treated with  $\text{Zn(Pc)}$  (left) or  $\text{Zr}^{\text{IV}}(\text{Pc})\text{Ac}_2$  (right) and rinsed with clean solvent. Full surface coverage by coordinated  $\text{Zr}^{\text{IV}}$  dye is indicated by EDAX spectra (see Supporting Information) and greater contrast, which also indicates greater dye loading on GO edge. The Zn dyes are completely removed by simple rinsing.

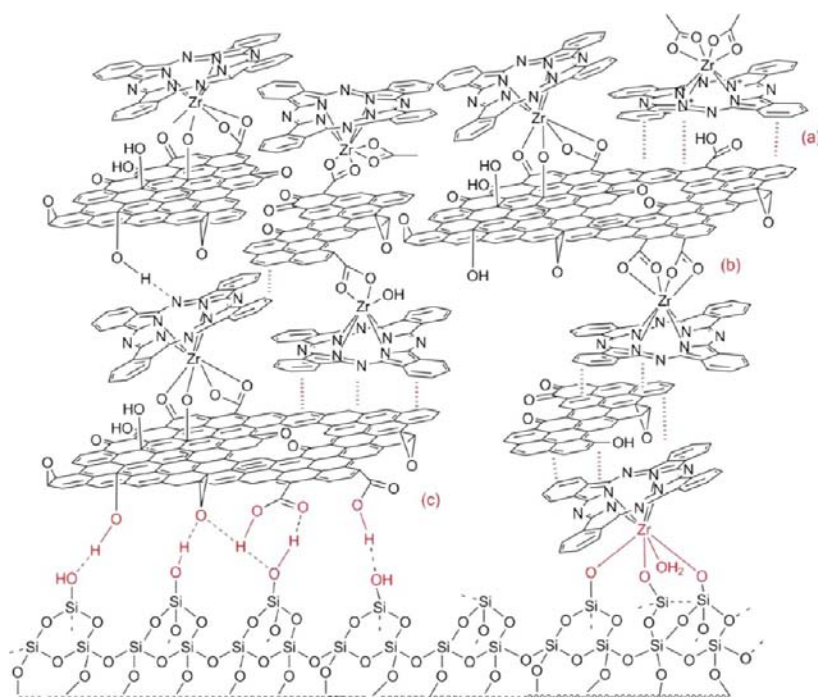


**Figure 7.** Representation of the possible intermolecular interactions between multilayers of dye-bound GO made by layer-by-layer methods. Interactions between the GO and  $\text{Zr}^{\text{IV}}(\text{Pc})$  on the quartz substrate include (a)  $\pi$ - $\pi$  interactions between the starting  $\text{Zr}^{\text{IV}}(\text{Pc})\text{Ac}_2$ , (b) coordination of the protruding  $\text{Zr}^{\text{IV}}$  ion of the  $\text{Pc}$  to the oxygen groups on GO, and (c) H-bonds between the substrate and the GO. The higher density of oxygen groups at the edges of GO result in greater binding of the  $\text{Zr}^{\text{IV}}$  dyes, see Figure 5. Other variations of these interactions are also present, for example, H-bond and  $\pi$ - $\pi$  interactions between GO flakes, see Supporting Information, Figure S13.

hybridized carbon allowing for layer growth mediated by the GO, but with small amounts of the dye entrained within the layers.  $\text{Zr}^{\text{IV}}(\text{Pc})$  and  $\text{ZrCl}_4$  both coordinate to the oxygenated regions of the GO.<sup>8</sup> Binding of the chromophores and the addition of new layers of GO are indicated by the linear increase of absorbance from the dyes and GO in the UV-visible spectra of the films. (Supporting Information, Figure S15). Though individual layers are incomplete, sequential dipping of the substrate into the GO and  $\text{Zr}^{\text{IV}}$  dye solutions builds nanofilms with controlled thickness, controlled optical density, and controlled coverage. As observed in dye-coated GO dispersions, binding of the  $\text{Zr}^{\text{IV}}$  dyes to the GO significantly diminishes the propensity of the GO to interact and results in only a gradual increase in film thickness as the

substrate is sequentially dipped in the solutions. We observed that the bound dye molecules also serve as nucleation points for the formation of microcrystals of dye, suggesting that GO might serve as a good substrate to grow microcrystals of other species. The highly varied composition of the GO affords many possible binding modes and binding sites for the  $\text{Zr}^{\text{IV}}$  dyes, for interactions between flakes of the GO, and for interactions with the substrate. The hydrophobic Zn dyes can interact with graphene like areas of the GO, while the oxophilic metal center can interact with oxygen functional groups on the GO and with the substrate.

## CONCLUSIONS

Self-organization of a composite film of Zr<sup>IV</sup> porphyrins or Zr<sup>IV</sup> phthalocyanines on GO is accomplished by the concomitant coordination of the metal ion to both the dye and the carboxylate groups decorating the edges of the GO sheets and the OH groups on the planar surfaces of GO. This supramolecular approach affords a material with high surface coverage of the dyes on the GO substrate and better electronic coupling of the two systems compared to porphyrinoids attached to GO by covalent chemistry. The hybrid material displays photonic properties derived from both the dyes and the GO.<sup>12</sup> Reduced GO has enhanced electronic properties, and the Zr<sup>IV</sup> dyes should bind to remaining oxygen containing defect sites.<sup>53</sup> This type of direct sensitization will broaden the applications of GO and foster the creation of new composite functional materials using cost-effective components and self-organization to create functional films.<sup>54–58</sup> These studies also indicate that the GO may serve as a means to grow microcrystals of other species.

## ASSOCIATED CONTENT

### Supporting Information

AFM, TEM, optical spectroscopy, control studies with Zn dyes, electronic measurements. This material is available free of charge via the Internet at <http://pubs.acs.org>.

## AUTHOR INFORMATION

### Corresponding Author

\*E-mail: [cdrain@hunter.cuny.edu](mailto:cdrain@hunter.cuny.edu). Phone: 212-650-3791.

### Author Contributions

The manuscript was written through contributions of all authors. All authors have given approval to the final version of the manuscript.

### Author Contributions

<sup>||</sup>These authors contributed equally.

### Notes

The authors declare no competing financial interest.

## ACKNOWLEDGMENTS

Supported by the U.S. National Science Foundation (NSF) CHE-0847997 and 1213962 to C.M.D. Hunter College science infrastructure is supported by the NSF, the National Institute on Minority Health and Health Disparities (8G12 MD007599) from the National Institutes of Health, and the City University of New York. We thank Jacopo Samson for his work with TEM and EDAX spectra, Ivana Radivojevic for the Zr<sup>IV</sup> dyes, and David Nissenbaum for help with figures.

## ABBREVIATIONS

GO, graphene oxide; TPP, 5,10,15,20-tetraphenylporphyrin; Pc, phthalocyanine; TEM, transmission electron microscopy; AFM, atomic force microscopy

## REFERENCES

- (1) Loh, K. P.; Bao, Q.; Eda, G.; Chhowalla, M. *Nat. Chem.* **2010**, *2*, 1015–1024.
- (2) Chen, D.; Feng, H.; Li, J. *Chem. Rev.* **2012**, *112*, 6027–6053.
- (3) Wan, X.; Huang, Y.; Chen, Y. *Acc. Chem. Res.* **2012**, *45*, 598–607.
- (4) Georgakilas, V.; Otyepka, M.; Bourlinos, A. B.; Chandra, V.; Kim, N.; Kemp, K. C.; Hobza, P.; Zboril, R.; Kim, K. S. *Chem. Rev.* **2012**, *112*, 6156–6214.

- (5) (a) Dreyer, D. R.; Park, S.; Bielawski, C. W.; Ruoff, R. S. *Chem. Soc. Rev.* **2010**, *39*, 228–240. (b) Park, S.; Ruoff, R. S. *Nat. Nanotechnol.* **2009**, *4*, 217–224.
- (6) Rourke, J. P.; Pandey, P. A.; Moore, J. J.; Bates, M.; Kinloch, I. A.; Young, R. J.; Wilson, N. R. *Angew. Chem., Int. Ed.* **2011**, *50*, 3173–3177.
- (7) Lurf, A.; He, H.; Forster, M.; Klinowski, J. *J. Phys. Chem. B* **1998**, *102*, 4477–4482.
- (8) Kim, J.; Cote, L. J.; Kim, F.; Yuan, W.; Shull, K. R.; Huang, J. *J. Am. Chem. Soc.* **2010**, *132*, 8180–8186.
- (9) Melucci, M.; Durso, M.; Zambianchi, M.; Treossi, E.; Xia, Z.-Y.; Manet, I.; Giambastiani, G.; Ortolani, L.; Morandi, V.; De Angelis, F.; Palermo, V. *J. Mater. Chem.* **2012**, *22*, 18237–18243.
- (10) Liu, Z.; Robinson, J. T.; Sun, X.; Dai, H. *J. Am. Chem. Soc.* **2008**, *130*, 10876–10877.
- (11) Sun, X.; Liu, Z.; Welscher, K.; Robinson, J.; Goodwin, A.; Zaric, S.; Dai, H. *Nano Res.* **2008**, *1*, 203–212.
- (12) Luo, Z.; Vora, P. M.; Mele, E. J.; Johnson, A. T. C.; Kikkawa, J. M. *Appl. Phys. Lett.* **2009**, *94*, 111909.
- (13) Shih, C.-J.; Lin, S.; Sharma, R.; Strano, M. S.; Blankschtein, D. *Langmuir* **2011**, *28*, 235–241.
- (14) Yang, Y.; Zhang, Y.-M.; Chen, Y.; Zhao, D.; Chen, J.-T.; Liu, Y. *Chem.—Eur. J.* **2012**, *18*, 4208–4215.
- (15) Yao, C.; Yan, L.-K.; Guan, W.; Liu, C.-G.; Song, P.; Su, Z.-M. *Dalton Trans.* **2010**, *39*, 7645–7649.
- (16) Arnold, M. S.; Zimmerman, J. D.; Renshaw, C. K.; Xu, X.; Lunt, R. R.; Austin, C. M.; Forrest, S. R. *Nano Lett.* **2009**, *9*, 3354–3358.
- (17) Tung, V. C.; Huang, J.-H.; Tevis, I.; Kim, F.; Kim, J.; Chu, C.-W.; Stupp, S. I.; Huang, J. *J. Am. Chem. Soc.* **2011**, *133*, 4940–4947.
- (18) Tung, V. C.; Kim, J.; Cote, L. J.; Huang, J. *J. Am. Chem. Soc.* **2011**, *133*, 9262–9265.
- (19) Yan, J.-M.; Wang, Z.-L.; Wang, H.-L.; Jiang, Q. *J. Mater. Chem.* **2012**, *22*, 10990–10993.
- (20) Xu, Y.; Liu, Z.; Zhang, X.; Wang, Y.; Tian, J.; Huang, Y.; Ma, Y.; Zhang, X.; Chen, Y. *Adv. Mater.* **2009**, *21*, 1275–1279.
- (21) Karousis, N.; Sandanayaka, A. S. D.; Hasobe, T.; Economopoulos, S. P.; Sarantopoulou, E.; Tagmatarchis, N. *J. Mater. Chem.* **2011**, *21*, 109–117.
- (22) Bala Murali Krishna, M.; Venkatramiah, N.; Venkatesan, R.; Narayana Rao, D. *J. Mater. Chem.* **2012**, *22*, 3059–3068.
- (23) Melucci, M.; Treossi, E.; Ortolani, L.; Giambastiani, G.; Morandi, V.; Klar, P.; Casiraghi, C.; Samori, P.; Palermo, V. *J. Mater. Chem.* **2010**, *20*, 9052–9060.
- (24) Pandey, P. A.; Rochford, L. A.; Keeble, D. S.; Rourke, J. P.; Jones, T. S.; Beanland, R.; Wilson, N. R. *Chem. Mater.* **2012**, *24*, 1365–1370.
- (25) Chunder, A.; Pal, T.; Khondaker, S. I.; Zhai, L. *J. Phys. Chem. C* **2010**, *114*, 15129–15135.
- (26) Malig, J.; Jux, N.; Kiessling, D.; Cid, J.-J.; Vázquez, P.; Torres, T.; Guldi, D. M. *Angew. Chem., Int. Ed.* **2011**, *50*, 3561–3565.
- (27) (a) Cárdenas-Jirón, G. I.; Leon-Plata, P.; Cortes-Arriagada, D.; Seminario, J. M. *J. Phys. Chem. C* **2011**, *115*, 16052–16062. (b) Zhang, X.-F.; Xi, Q. *Carbon* **2011**, *49*, 3842–3850.
- (28) Wang, X.; Zhi, L.; Mullen, K. *Nano Lett.* **2007**, *8*, 323–327.
- (29) Zhong, S.; Zhong, J. Q.; Mao, H. Y.; Wang, R.; Wang, Y.; Qi, D. C.; Loh, K. P.; Wee, A. T. S.; Chen, Z. K.; Chen, W. *ACS Appl. Mater. Interfaces* **2012**, *4*, 3134–3140.
- (30) Park, H.; Howden, R. M.; Barr, M. C.; Bulović, V.; Gleason, K.; Kong, J. *ACS Nano* **2012**, *6*, 6370–6377.
- (31) Poursaberi, T.; Hassaniadi, M. *J. Porphyrins Phthalocyanines* **2012**, *16*, 1140–1147.
- (32) Brand, H.; Arnold, J. *Coord. Chem. Rev.* **1995**, *140*, 137–168.
- (33) Falber, A.; Burton-Pye, B. P.; Radivojevic, I.; Todaro, L.; Saleh, R.; Francesconi, L. C.; Drain, C. M. *Eur. J. Inorg. Chem.* **2009**, *2009*, 2459–2466.
- (34) Radivojevic, I.; Bazzan, G.; Burton-Pye, B. P.; Ithisuphalap, K.; Saleh, R.; Durstock, M. F.; Francesconi, L. C.; Drain, C. M. *J. Phys. Chem. C* **2012**, *116*, 15867–15877.

- (35) Radivojevic, I.; Burton-Pye, B. P.; Saleh, R.; Ithisuphalap, K.; Francesconi, L. C.; Drain, C. M. *RSC Adv.* **2013**, *3*, 2174–2177.
- (36) Liao, M.-S.; Scheiner, S. J. *Chem. Phys.* **2002**, *117*, 205–219.
- (37) Varotto, A.; Nam, C.-Y.; Radivojevic, I.; P. C. Tomé, J.; Cavaleiro, J. A. S.; Black, C. T.; Drain, C. M. *J. Am. Chem. Soc.* **2010**, *132*, 2552–2554.
- (38) Paredes, J. I.; Villar-Rodil, S.; Martínez-Alonso, A.; Tascón, J. M. D. *Langmuir* **2008**, *24*, 10560–10564.
- (39) Zhang, L.; Xia, J.; Zhao, Q.; Liu, L.; Zhang, Z. *Small* **2010**, *6*, 537–544.
- (40) Yamaguchi, H.; Murakami, K.; Eda, G.; Fujita, T.; Guan, P.; Wang, W.; Gong, C.; Boisse, J.; Miller, S.; Acik, M.; Cho, K.; Chabal, Y. J.; Chen, M.; Wakaya, F.; Takai, M.; Chhowalla, M. *ACS Nano* **2011**, *5*, 4945–4952.
- (41) Zhu, Y.; Li, X.; Cai, Q.; Sun, Z.; Casillas, G.; Jose-Yacaman, M.; Verduzco, R.; Tour, J. M. *J. Am. Chem. Soc.* **2012**, *134*, 11774–11780.
- (42) Treossi, E.; Melucci, M.; Liscio, A.; Gazzano, M.; Samori, P.; Palermo, V. *J. Am. Chem. Soc.* **2009**, *131*, 15576–15577.
- (43) Bazzan, G.; Smith, W.; Francesconi, L. C.; Drain, C. M. *Langmuir* **2008**, *24*, 3244–3249.
- (44) Quintana, M.; Montellano, A.; del Rio Castillo, A. E.; Tendeloo, G. V.; Bittencourt, C.; Prato, M. *Chem. Commun.* **2011**, *47*, 9330–9332.
- (45) Becerril, H. A.; Mao, J.; Liu, Z.; Stoltenberg, R. M.; Bao, Z.; Chen, Y. *ACS Nano* **2008**, *2*, 463–470.
- (46) Li, D.; Muller, M. B.; Gilje, S.; Kaner, R. B.; Wallace, G. G. *Nat. Nano* **2008**, *3*, 101–105.
- (47) Thomas, H. R.; Valles, C.; Young, R. J.; Kinloch, I. A.; Wilson, N. R.; Rourke, J. P. *J. Mater. Chem. C* **2013**, *1*, 338–342.
- (48) Eda, G.; Fanchini, G.; Chhowalla, M. *Nat. Nanotechnol.* **2008**, *3*, 270–274.
- (49) Jin, M.; Jeong, H.-K.; Yu, W. J.; Bae, D. J.; Kang, B. R.; Lee, Y. H. *J. Phys. D: Appl. Phys.* **2009**, *42*, 135109.
- (50) Chang, C.-H.; Fan, X.; Li, L.-J.; Kuo, J.-L. *J. Phys. Chem. C* **2012**, *116* (25), 13788–13794.
- (51) Kovtyukhova, N. I.; Ollivier, P. J.; Martin, B. R.; Mallouk, T. E.; Chizhik, S. A.; Buzaneva, E. V.; Gorchinskiy, A. D. *Chem. Mater.* **1999**, *11*, 771–778.
- (52) Zhao, X.; Zhang, Q.; Hao, Y.; Li, Y.; Fang, Y.; Chen, D. *Macromolecules* **2010**, *43*, 9411–9416.
- (53) Luo, D.; Zhang, G.; Liu, J.; Sun, X. *J. Phys. Chem. C* **2011**, *115*, 11327–11335.
- (54) Beletskaya, I.; Tyurin, V. S.; Tsivadze, A. Y.; Guillard, R.; Stern, C. *Chem. Rev.* **2009**, *109*, 1659–1713.
- (55) Drain, C. M.; Varotto, A.; Radivojevic, I. *Chem. Rev.* **2009**, *109*, 1630–1658.
- (56) Radivojevic, I.; Varotto, A.; Farley, C.; Drain, C. M. *Energy Environ. Sci.* **2010**, *3*, 1897–1909.
- (57) Drain, C. M.; Bazzan, G.; Milic, T.; Vinodu, M.; Goeltz, J. C. *Israel J. Chem.* **2005**, *45*, 255–269.
- (58) Jurow, M. J.; Hageman, B. A.; DiMasi, E.; Nam, C.-Y.; Pabon, C.; Black, C. T.; Drain, C. M. *J. Mater. Chem. A* **2013**, *1*, 1557–1565.